fractal and fractional

MDPI

Article

Optimizing Gas Flooding with Fractal Theory for Water Coning Suppression and Oil Recovery Enhancement

Baolei Liu [1,2,3,4,*], Kai Chen [4] and Xiaojie Zheng [5]

[1] Key Laboratory of Exploration Technologies for Oil and Gas Resources (Yangtze University), Ministry of Education, Wuhan 430100, China
[2] State Key Laboratory of Low Carbon Catalysis and Carbon Dioxide Utilization (Yangtze University), Wuhan 430100, China
[3] Hubei Key Laboratory of Oil and Gas Drilling and Production Engineering (Yangtze University), Wuhan 430100, China
[4] School of Petroleum Engineering, Yangtze University, Wuhan 430100, China; 15399719377@163.com
[5] Sinopec Group Northwest Petroleum Branch, Urumqi 830011, China; zhengxj.xbsj@sinopec.com
* Correspondence: baoleiliu@yangtzeu.edu.cn; Tel.: +86-18163551062

Abstract

This study addresses high water cut and low recovery in bottom-water sandstone reservoirs by optimizing CO_2 and N_2 foam flooding parameters. The key innovation is the pioneering application of fractal dimension to quantitatively characterize water coning morphology during composite gas flooding. A numerical simulation assessed composite gas type, injection gas ratio, sequence, speed, volume, and injection–production ratio. Fractal dimension quantified water coning. Optimal conditions were: 2:1 injection gas ratio (CO_2 then N_2 foam), 140 t/d injection speed, 0.31 PV volume, and 1:3.2 injection–production ratio. This achieved 39.52% recovery over 15 years—a 4.89% increase, adding 3.17×10^4 t of oil. Fractal dimension fell to 1.672. Sensitivity analysis showed the injection gas ratio most affects oil output. The injection volume best suppresses water coning. The injection speed has low sensitivity. Key interactions exist between volume, gas type, and injection–production ratio. Injection gas ratio, volume, and injection–production ratio are crucial for development control. The proposed methodology presents a viable strategy for enhancing oil recovery in similar reservoirs, with broader implications for advancing CO_2 utilization and supporting carbon management objectives in the petroleum industry.

Keywords: optimization of gas injection parameters; composite gas flooding; fractal dimension; sensitivity analysis; reservoir numerical simulation; sandstone reservoirs with bottom water

Check for updates

Academic Editor: Kouqi Liu

Received: 28 January 2026
Revised: 26 February 2026
Accepted: 2 March 2026
Published: 4 March 2026

Copyright: © 2026 by the authors. Licensee MDPI, Basel, Switzerland. This article is an open access article distributed under the terms and conditions of the Creative Commons Attribution (CC BY) license.

1. Introduction

The development of bottom-water sandstone oil reservoirs is confronted with problems such as strong bottom-water cone advancement, early water flooding, and prominent reservoir heterogeneity, which lead to a rapid increase in water cut, severe water flooding of oil wells, and a sharp decline in production, making stable production difficult. Water coning is a common production problem where underlying water rises toward the production well due to pressure drawdown, forming a cone-shaped interface that eventually leads to premature water breakthrough and reduced oil recovery. Gas injection technology, with its unique advantages, has become an important means to improve the development effect. The injected gas forms a dynamic gas barrier at the oil–water interface through gravity

segregation, actively inhibiting the rise in bottom water, while improving the fluidity of crude oil. In a single gas drive, only one type of gas (e.g., CO_2 alone or N_2 alone) is injected. In a composite gas drive, two or more gases or gas-based fluids (e.g., CO_2 followed by N_2 foam) are injected in sequence to leverage their complementary mechanisms. Among them, the composite gas drive, through the synergistic effect of multiple media, shows a more significant potential for water control and oil increase compared to a single gas drive.

In recent years, gas injection-enhanced oil recovery techniques have been extensively implemented in various reservoir types. Existing research can be thematically grouped based on the dominant injection mechanisms and gas compositions.

1.1. CO_2-Based Gas Injection

CO_2 injection technology has become an important research direction for enhancing oil recovery due to its good miscibility and crude oil expansion effect. In the aspect of CO_2 and N_2 combined flooding, Ziyan Li et al. [1] used a dual-porosity dual-permeability model to optimize the mixing ratio of CO_2 and N_2, which not only increased the recovery rate of shale gas but also enhanced the CO_2 sequestration effect. Zongfa Li et al. [2] further clarified the synergy mechanism between the two: CO_2 causes crude oil expansion and reservoir depressurization, while N_2 maintains pressure, and the combination of the two can significantly increase the recovery rate. Fang et al. [3] systematically evaluated the impact of the CO_2/N_2 molar ratio on oil displacement efficiency, indicating that the oil displacement efficiency increases with the increase in CO_2 concentration, and the optimal injection method is to inject a CO_2 slug first, followed by N_2. Tao Yu et al. [4] revealed from a microscopic mechanism that the expansion and viscosity reduction in CO_2, combined with the pressure support of N_2, can transform capillary force from flow resistance to oil displacement force, and together with the Jamin effect, promote the mobilization of remaining oil.

In the aspect of CO_2 and CH_4 combined flooding, Pengcheng Liu et al. [5] studied the effect of CO_2-CH_4 alternate gas–water flooding in rhythmic reservoirs through numerical simulation and found that due to the density difference in the fluids, this method is most effective in homogeneous reservoirs, followed by positive rhythmic reservoirs, and least effective in negative rhythmic reservoirs. Jinhyung Cho et al. [6] established a simulation model considering asphaltene deposition and found that although the addition of CH_4 reduces the phase solubility of the system, its effect in mitigating asphaltene deposition can offset this impact, and the final recovery rate is higher than that of pure CO_2 flooding.

1.2. Nitrogen and Flue Gas

Nitrogen and flue gas, mainly composed of nitrogen, show good potential under specific reservoir conditions. Zhouhua Wang et al. [7], based on long core experiments, found that alternate injection of flue gas and water can increase the recovery rate by about 21.25% compared to continuous water flooding. Serdar Bender and Haishui Han et al. [8,9], through experiments, simulations, and field practices, systematically verified the effectiveness of flue gas in driving oil in gravel-filled reservoirs. Wanli Kang et al. [10] pointed out that air injection technology (mainly composed of nitrogen) has achieved significant benefits in shallow low-permeability oil reservoirs, increasing the crude oil recovery rate from 37% to 48% in a certain oilfield in the North Sea.

1.3. Mixed Gases and Hydrocarbon Gases

Tian Ye et al. [11] used a component model to compare different gas injection schemes and found that rich gas-mixed gases can achieve better development effects. Matthew Monette et al. [12] studied the impact of hydrocarbon gas components in low-permeability reservoirs on the formation of microemulsions and crude oil expansion, indicating that the

comprehensive production enhancement effect is more obvious. Alireza Qazvini Firouz et al. [13] pointed out that a ternary mixture of methane, nitrogen, and carbon dioxide can significantly increase the recovery rate, with the optimal CO_2 content being 10–25%.

1.4. Optimization Through Experimental Design

The application of experimental design methods provides a systematic and rigorous research approach for optimizing parameters in gas flooding for enhanced oil recovery. Shokufe Afzali et al. [14] used multi-scale experiments such as core flooding and microscopic models to optimize injection parameters such as the number of cycles and injection mode, verifying the key role of parameter optimization in enhancing recovery rate. Watheq J. Al-Mudhafar et al. [15–18] optimized CO_2 injection rate, injection mode, and cycle through high-resolution geostatistical modeling, Latin hypercube sampling, radial basis function neural networks, and machine learning algorithms, combined with numerical simulation. Mahmoud et al. [19] used a glass visual model to optimize CO_2 injection rate, injection mode, and injection depth.

Although the aforementioned research has achieved significant progress in the development of bottom-water sandstone reservoirs, core problems such as intense bottom-water penetration, irregular front morphology, and prominent heterogeneity are commonly encountered, leading to premature water flooding of oil wells, rapid increases in water content, and low recovery rates. The existing research still has certain limitations: the front edge of bottom-water penetration exhibits multi-scale self-similar irregular expansion characteristics. Traditional characterization methods (such as water content and oil production volume as macroscopic indicators) can only reflect the final result of penetration, but cannot accurately capture the dynamic evolution process of the front edge morphology. The core advantage of fractal theory lies in the ability to convert the morphological characteristics of irregular geometric bodies into quantifiable numerical values, which precisely match the self-similarity and irregularity of bottom-water penetration. However, previous studies have not introduced fractal dimension into the characterization of water cone shape in the composite gas drive process, resulting in the lack of a precise quantitative basis for evaluating the inhibition effect of bottom-water penetration. Therefore, the core innovation of this study lies in introducing fractal dimension into the characterization of bottom-water cone penetration in the composite gas drive process and converting the vague goal of "suppressing bottom water penetration" into a clear quantitative indicator. Combined with reservoir numerical simulation and global sensitivity analysis, it provides a new solution for the efficient development of bottom-water sandstone reservoirs.

2. Reservoir Modeling and Fractal Characterization

2.1. Overview of Reservoir

The T oil reservoir in the Tahe Oilfield is a classic blocky bottom-water sandstone reservoir, characterized by three principal development challenges: a thin pay zone, a potent bottom-water aquifer with a water–oil ratio exceeding 500:1, and significant heterogeneity evidenced by a permeability variation coefficient of 0.87–1.04. As of end-2023, the original oil in place was 1.06×10^7 t, with cumulative production of 3.85×10^6 t, yielding a 36.3% recovery factor. The field's 55 wells produce 5×10^3 t/d of liquid and 1.6×10^2 t/d of oil, with a 96.7% water cut and a marginal average of 4.1 t/d per well, indicating a mature development stage requiring enhanced recovery measures. The reservoir model is shown in Figure 1.

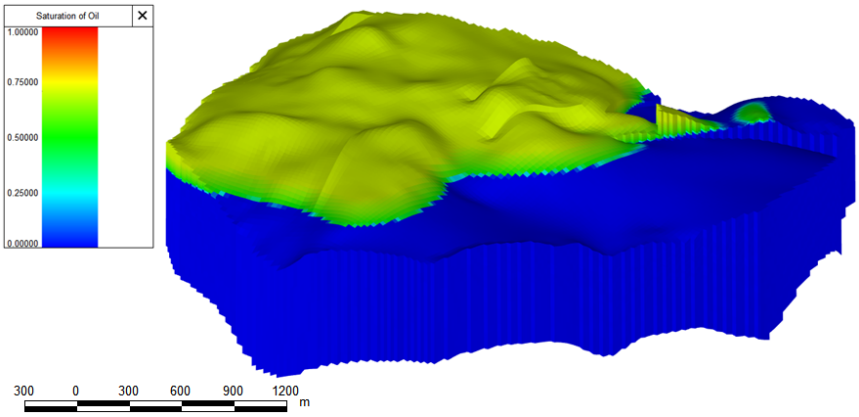


Figure 1. Reservoir schematic diagram.

2.2. Establishment of Numerical Model

A numerical model has been developed that reflects the characteristics of a standard block from the T oil reservoir. The model parameters combine field-measured data (depth: 3647 m, temperature: 110 °C, and initial pressure: 50.18 MPa) with representative model values (averaged porosity: 22%, planar permeability: 350 mD, and longitudinal permeability: 125 mD). The three-dimensional model is comprehensively outlined in Table 1, which specifies a grid size of 25 m × 25 m, culminating in a total of 50,654 grids (43 × 31 × 38). The specific physical property parameters pertinent to the model are depicted in Figure 2. This model consists of three wells with fixed roles throughout the simulation: W2 is a dedicated gas injection well, while W1 and W3 are production wells. In the simulation, W2 continuously injects the composite gas according to a predefined sequence, rate, and volume, while W1 and W3 produce fluids simultaneously under a constant liquid rate constraint subject to a minimum bottom-hole pressure limit. It is projected that the operational lifespan of the oilfield will extend over a period of 15 years.

Table 1. Parameters of the numerical model for the T oil reservoir.

Parameters	Values
Reference depth/m	3647
Temperature/°C	110
Pressure/MPa	50.18
Porosity/%	22
Planar permeability/mD	350
Longitudinal permeability/mD	125

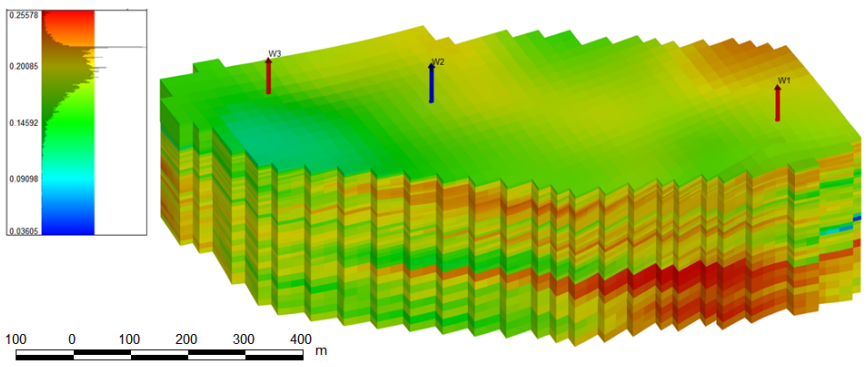


Figure 2. Three-dimensional numerical model of the T oil reservoir.

2.3. Fractal Analysis of Water Coning Morphology

Fractal theory provides a powerful mathematical framework for characterizing the multi-scale heterogeneous features of complex systems. It has found unique application value in petroleum engineering for describing irregular geometries and spatial structures. Previous work has focused on characterizing pore structures using 3D CT technology [20], predicting fracture network permeability [21], developing fractal–fractional diffusion models for fractured wells [22], and constructing multi-scale flow models for shale reservoirs [23–25]. Recent applications of fractal theory have further extended to dynamic transport processes in complex porous media. However, the application of fractal theory has predominantly been confined to describing static pore structures and fracture networks or modeling flow in unconventional reservoirs, but no quantitative analysis has been conducted for the dynamic front of bottom-water penetration. Regarding the irregular and self-similar expansion characteristics of bottom-water penetration in T reservoirs, traditional methods can only indirectly infer the degree of penetration and cannot quantify the spatial distribution and dynamic changes in the front shape, making it difficult to accurately evaluate the inhibitory effect of gas injection parameters. Given the irregular and self-similar characteristics typically exhibited by the advancing bottom-water cone, fractal theory is particularly suitable for its description. The core value of fractal dimension lies in converting the morphological characteristics of bottom-water penetration into quantifiable numerical values and providing a direct target for optimizing gas injection parameters. The specific method is as follows.

By analyzing the water saturation field diagrams output by the numerical simulation software, the geometric shape of the water coning front was extracted. For fractal analysis, the extracted shape underwent a standardized image-processing procedure to ensure reproducibility. First, the image was converted to a binary format using a method for automatic thresholding, which optimally separates the coning structure from the background. The resulting binary image was then used for fractal dimension calculation via the box-counting method (Equation (1)). In this process, a series of grids with box sizes (ε) ranging from 2 to 64 pixels (in powers of 2) were overlaid on the binary image. For each box size ε, the number of boxes $N(\varepsilon)$ containing part of the coning front was counted. The fractal dimension D was finally determined as the absolute slope of the linear regression line fitted to the data points in the $\log N(\varepsilon)$ versus $\log(1/\varepsilon)$ plot. A dimension closer to the Euclidean plane limit of two indicates more significant water coning, while lower values correspond to flatter, more suppressed coning morphology as shown in Figure 3. The fractal dimension D typically ranges between 1 and 2, with the upper limit representing extreme geometric complexity; it characterizes spatial distribution rather than average saturation and thus has no simple linear relationship with water saturation:

$$D = \lim_{\varepsilon \to 0} \frac{\log N(\varepsilon)}{\log(1/\varepsilon)} \tag{1}$$

where:

ε: size of the box.

$N(\varepsilon)$: minimum number of boxes required to cover the leading edge of the bottom-water cone.

D: fractal dimension.



(**a**) (**b**)

Figure 3. Binary images of the extracted bottom-water cone front used for fractal dimension calculation via the box-counting method. (**a**) Suppressed water cone with a lower fractal dimension (D = 1.692), indicating a flatter and more uniform front morphology. (**b**) Severe water coning with a higher fractal dimension (D = 1.793), showing a more irregular and fingered front.

3. Parameter Optimization and Mechanism Analysis

3.1. Optimization of Injection Parameters

Based on the core concept of quantifying conical shapes through fractal dimensions, numerical simulations were conducted to optimize the parameters of the composite gas drive. The optimization goal was to maximize the cumulative oil production and minimize the fractal dimension. The optimization of injection parameters was conducted sequentially for the six key parameters: composite gas type, injection sequence, gas injection ratio, injection speed, injection volume, and injection–production ratio. During the optimization of one parameter, the others were set to default values. These default values were chosen based on common field practices and preliminary simulation results to ensure they represent a realistic and stable operation. The optimal value obtained for each parameter was then fixed for the subsequent parameter optimization. There are three composite gas injection types: carbon dioxide and nitrogen foam, nitrogen foam and methane, and carbon dioxide and methane. The optimization of the composite gas type is integrated within the analysis of the injection sequence, as the latter directly compares the performance of different gas type combinations. After determining the optimal composite gas type and the optimal injection sequence, these values were fixed for the subsequent optimization of the remaining parameters. The gas injection sequence has been set up with six options, as summarized in Table 2.

Table 2. Summary of the six injection sequence options.

Option	Injection Sequence
1	CO_2 followed by N_2 foam
2	N_2 foam followed by CO_2
3	N_2 foam followed by CH_4
4	CH_4 followed by N_2 foam
5	CO_2 followed by CH_4
6	CH_4 followed by CO_2

After fixing the optimal composite gas type (CO_2 and N_2 foam) and the optimal injection sequence (CO_2 followed by N_2 foam), the remaining parameters—gas injection ratio, injection speed, injection volume, and injection–production ratio—were optimized sequentially. The gas injection ratio refers to the volume ratio of CO_2 to N_2 foam. The results for each parameter are summarized in Figures 4–8.

The simulation results identified the optimal configuration as the combination of CO_2 and N_2 foam, injected in a sequence of CO_2 followed by N_2 foam, with a gas ratio of 2:1, an injection speed of 100 t per day, an injection volume of 0.25 pore volumes (PV), and an injection–production ratio of 1:3.5. The optimal values were determined by balancing cumulative oil production and fractal dimension.

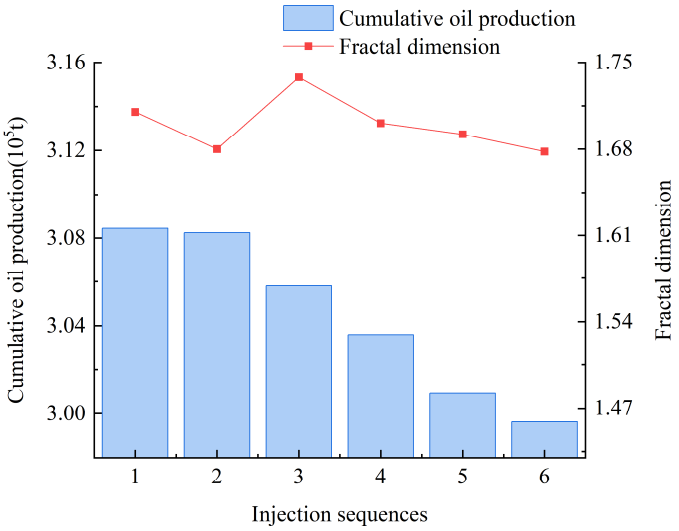


Figure 4. The influence of gas injection sequence on cumulative oil production and fractal dimension. The horizontal axis (Options 1–6) corresponds to the injection sequences defined in Table 2.

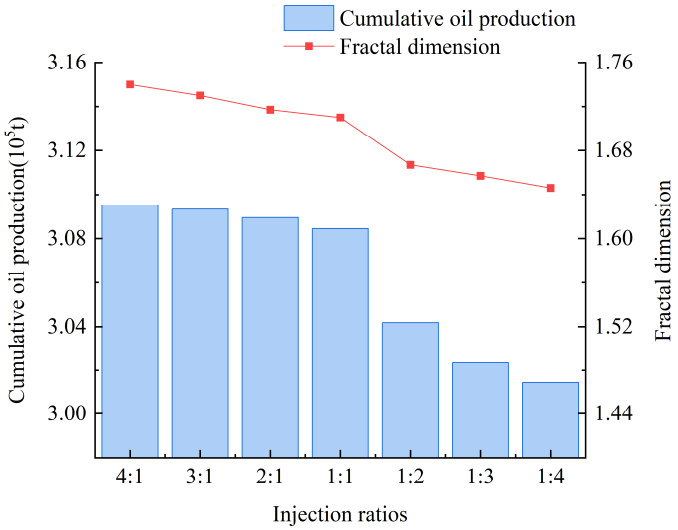


Figure 5. The influence of gas injection ratio on cumulative oil production and fractal dimension.

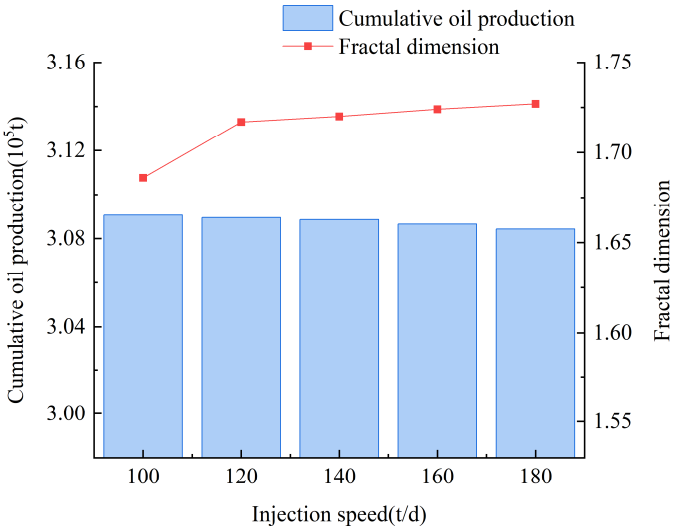


Figure 6. The influence of gas injection speed on cumulative oil production and fractal dimension.

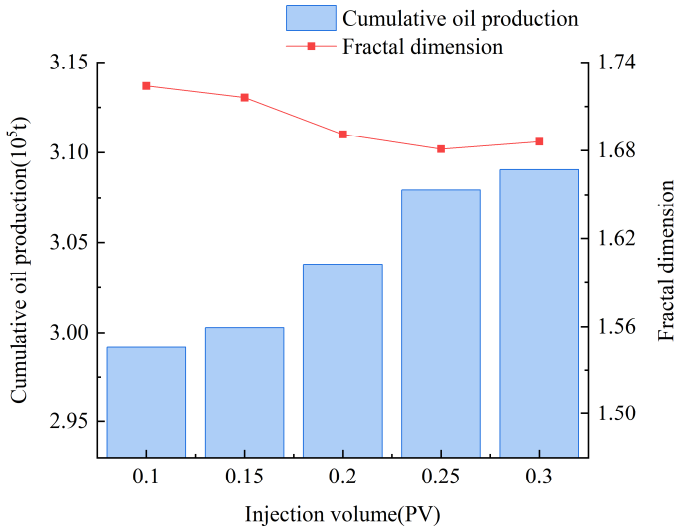


Figure 7. The influence of gas injection volume on cumulative oil production and fractal dimension.

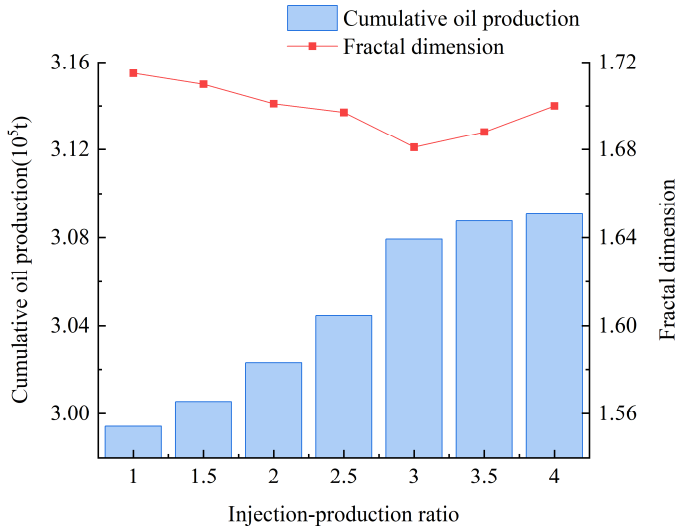


Figure 8. The influence of gas injection–production ratio on cumulative oil production and fractal dimension.

3.2. Dominant Mechanisms from Optimized Parameters

The mechanisms underlying the parameter effects are elucidated based on the trends observed in the single-factor analysis (Figures 4–8). These trends provide fundamental insights into the individual role of each parameter, which form the basis for understanding their behavior in the composite process.

The superior performance of the CO_2 + N_2 foam combination (Figure 4) stems from a synergistic effect. CO_2 effectively mixes with and swells the crude oil, enhancing its mobility, while the N_2 foam provides a robust physical barrier, selectively plugging high-permeability channels and suppressing water coning [26–31]. The optimal injection sequence of CO_2 preceding N_2 foam (Figure 4) allows the CO_2 to first contact and mobilize the oil. The subsequent N_2 foam then displaces this mobilized oil and reinforces the barrier against bottom water. Reversing this sequence would prematurely block the pores with foam, hindering the critical contact between CO_2 and the oil.

The optimal 2:1 injection gas ratio (Figure 5) strikes a critical balance between displacement efficiency and coning control. This ratio ensures a sufficient volume of CO_2 for effective oil mobilization and viscosity reduction, while maintaining an adequate foam strength to resist water breakthrough [32–36]. The lower injection speed of 100 t/d (Figure 6)

promotes better foam stability and provides longer contact time for CO_2–oil interaction, thereby improving sweep efficiency, unlike higher rates, which favor channeling through preferential paths.

The injection volume of 0.25 PV (Figure 7) represents a point of diminishing returns for oil recovery, beyond which contact with new oil becomes limited. However, a larger volume consistently strengthens the foam barrier, leading to better coning control, as evidenced by a steadily decreasing fractal dimension [37]. The injection–production ratio of 1:3.5 (Figure 8) optimally balances the need for sufficient energy to drive oil towards producers with the requirement to maintain reservoir pressure for foam barrier stability.

These mechanistic insights from single-factor trends provide a fundamental understanding for the multi-parameter optimization that follows.

4. Sensitivity Analysis and Discussion of Injection Parameters

4.1. Single-Factor Sensitivity Analysis

Single-factor sensitivity analysis evaluates the individual impact of each gas injection parameter on cumulative oil production and fractal dimension, using the *p*-value from significance tests and range analysis. The calculation is based on the following formulas:

$$t = \frac{|\mu_1 - \mu_2|}{\sqrt{\frac{{S_1}^2}{n_1} + \frac{{S_2}^2}{n_2}}} \tag{2}$$

$$P = f(t, df) \tag{3}$$

$$df = n_1 + n_2 - 2 \tag{4}$$

$$R_j = \max(Y_j) - \min(Y_j) \tag{5}$$

where:

μ_1, μ_2: output means at different parameter levels.
S_1, S_2: standard deviations.
n_1, n_2: sample sizes.
df: degree of freedom.
$f(t, df)$: t-distribution function.
R_j: extreme value of parameter j.
$\max(Y_j)$: maximum value among all the values of parameter j.
$\min(Y_j)$: minimum value among all the values of parameter j.

The single-factor analysis reveals significant interactions among parameters. Table 3 shows that injection type, sequence, and volume interact notably in affecting cumulative oil production. Similarly, Table 4 indicates that these parameters, along with injection speed, interact significantly in controlling the fractal dimension.

Table 3. Matrix table of significance *p*-values for cumulative oil production.

	Injection Type	Injection Gas Ratio	Injection Sequence	Injection Speed	Injection Volume	Injection–Production Ratio
Injection Type	0	1	0.001	0.191	0.017	0.314
Injection gas ratio	1	0	1	1	1	1
Injection sequence	0.001	1	0	0.151	0.008	0.269
Injection speed	0.191	1	0.151	0	0	0.1
Injection volume	0.017	1	0.008	0	0	0.102
Injection–production ratio	0.314	1	0.269	0.1	0.102	0

Table 4. Significance *p*-value matrix for fractal dimension.

	Injection Type	Injection Gas Ratio	Injection Sequence	Injection Speed	Injection Volume	Injection–Production Ratio
Injection Type	0	0.412	0.003	0.175	0.008	0.286
Injection gas ratio	0.412	0	0.725	0.837	0.623	0.901
Injection sequence	0.003	0.725	0	0.132	0.005	0.241
Injection speed	0.175	0.837	0.132	0	0.001	0.087
Injection volume	0.008	0.623	0.005	0.001	0	0.095
Injection–production ratio	0.286	0.901	0.241	0.087	0.095	0

The extreme difference analysis (Figure 9) further quantifies the parameter sensitivities. Injection volume has the most substantial impact on both cumulative oil production (range: 0.111) and fractal dimension (range: 0.085). This divergence stems from their different mechanistic roles: the injection gas ratio governs the balance between CO_2 miscible displacement and N_2 foam coning control, directly determining oil recovery efficiency, while injection volume determines the spatial scale and stability of the foam barrier against bottom water, thus controlling coning morphology.

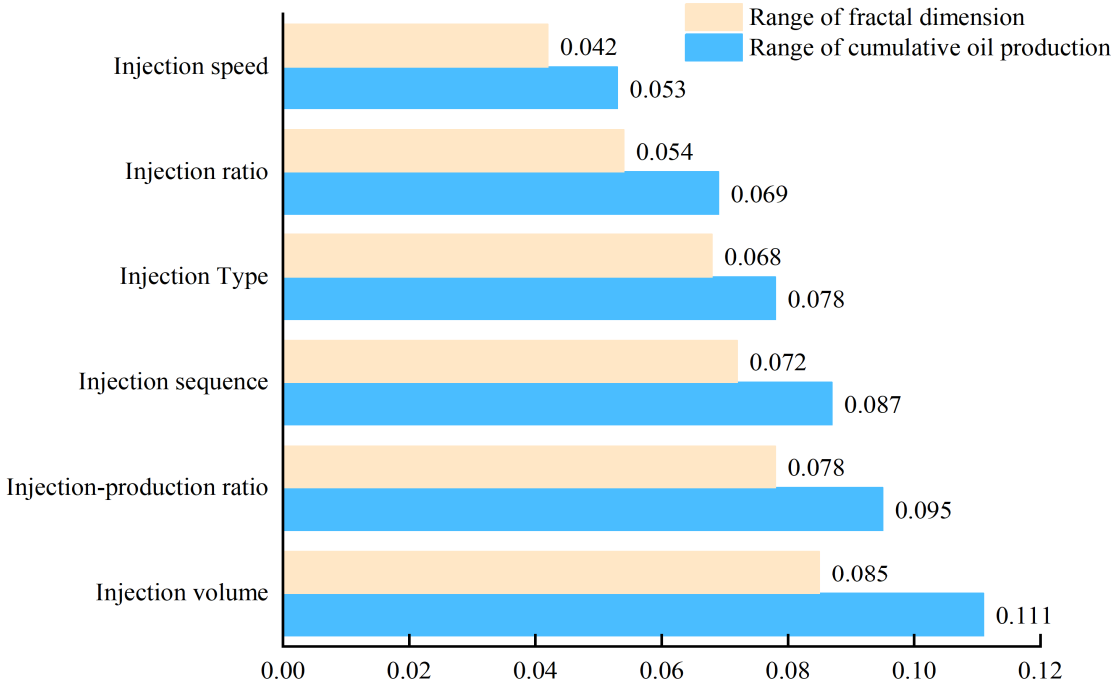


Figure 9. Analysis results of the extreme difference in gas injection parameters.

4.2. Global Sensitivity Analysis

Global sensitivity analysis using the Sobol index method quantifies the main and total effect indices of each parameter. The total effect index S_{T_i} is calculated as:

$$S_{T_i} = 1 - \frac{Var_{X_{\sim i}}\left[E_{X_i}(Y|X_{\sim i})\right]}{Var(Y)} \quad (6)$$

where:

S_{T_i}: total effect index of parameter i.

Y: cumulative oil production or fractal dimension.

X_i: the i-th parameter.

$X_{\sim i}$: all parameters except X_i.

$Var(Y)$: variance of the response variable Y.

$E_{X_i}(Y|X_{\sim i})$: conditional expectation obtained by taking the expectation of parameter X_i under the condition that all other parameters $X_{\sim i}$ are given.

As shown in Figure 10, the injection gas ratio exhibits the strongest main effect on cumulative oil production (S_1 = 0.31), confirming its primary role in balancing displacement efficiency, while injection volume dominates the fractal dimension (S_1 = 0.28), highlighting its critical function in coning suppression. The total effect indices (S_T) further confirm these parameters' overall influence, considering their interactions with others.

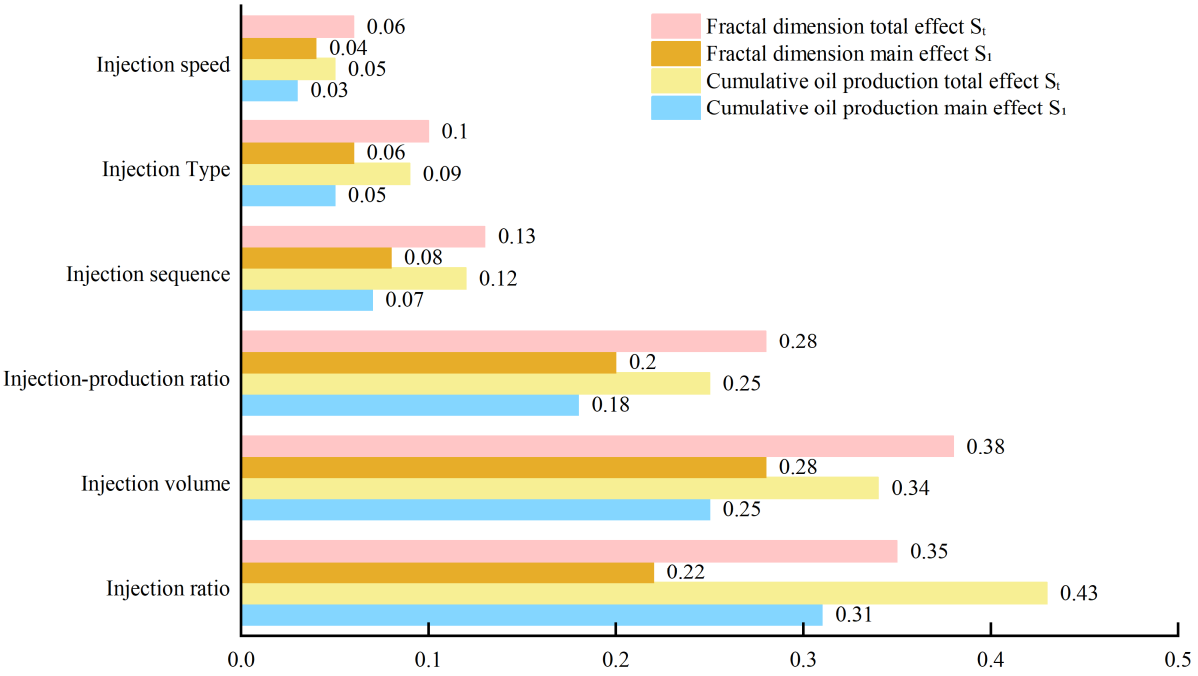


Figure 10. The results of the global sensitivity analysis.

4.3. Multi-Factor Interaction Analysis

The SHAP interaction method quantifies the synergistic or antagonistic effects between parameters. The interaction value φ_{ij} between parameters x_i and x_j is calculated as:

$$\varphi_{ij} = f(x_i, x_j) - f(x_i) - f(x_j) + f(\varnothing) \quad (7)$$

where:

φ_{ij}: interaction value between parameters i and j.

$f(x_i, x_j)$: output when both parameters i and j change simultaneously.

$f(x_i)$: output when only parameter i changes.

$f(\varnothing)$: output when all parameters take the reference value.

Figure 11 shows that the interaction between injection volume and gas type has the highest SHAP value for both responses. This strong interaction further explains the sensitivity patterns: The effectiveness of a specific gas type in improving displacement and coning control depends strongly on the injected volume, requiring coordinated optimization of these parameters.

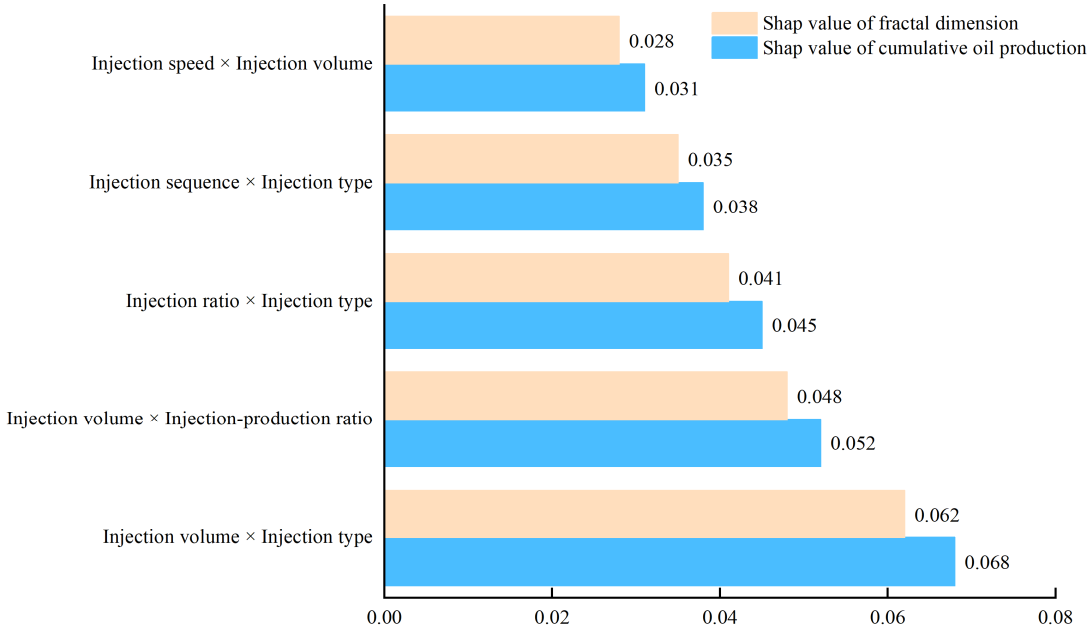


Figure 11. SHAP interaction value analysis results.

4.4. Sensitivity Ranking

Table 5 synthesizes the sensitivity rankings from all analyses. The distinct ranking patterns confirm the different mechanistic priorities: For cumulative oil production, the injection gas ratio ranks first due to its direct control over the displacement-blocking balance; for the fractal dimension, injection volume ranks first because it determines the scale of coning suppression. The injection–production ratio consistently ranks third, serving as a balancing factor between displacement energy and pressure maintenance.

Table 5. The sensitivity ranking results.

Parameter Name	Order of Sensitivity to Cumulative Oil Production	Order of Sensitivity to Fractal Dimension
Injection gas ratio	1	2
Injection volume	2	1
Injection–production ratio	3	3
Type of injected gas	4	4
Sequence of gas injection	5	5
Injection speed	6	6

The dominance of the injection gas ratio in determining oil recovery stems from its direct regulation of the balance between two key processes: CO_2 miscible displacement and N_2 foam coning control. An optimal ratio ensures sufficient CO_2 contact with the crude oil to achieve swelling and viscosity reduction, thereby enhancing displacement efficiency, while maintaining adequate foam strength to block high-permeability channels.

Conversely, injection volume plays a decisive role in suppressing water coning, as reflected by its top ranking for the fractal dimension. A larger injected volume extends the spatial distribution and enhances the stability of the foam barrier, thereby more effectively restraining the upward movement of the bottom water. This results in a flatter, more uniform water front, which is quantitatively captured by a lower fractal dimension.

Thus, the sensitivity ranking underscores a clear functional decoupling: The injection gas ratio is paramount for maximizing oil recovery by optimizing the displacement process, while the injection volume is crucial for controlling the coning morphology by establishing

a robust and extensive blocking zone. The injection–production ratio consistently ranks third, serving as a balancing factor between providing sufficient displacement energy and maintaining reservoir pressure for foam stability.

5. Optimization Application and Analysis

5.1. Optimal Scheme and Validation

Bayesian optimization identified the global optimum parameters for the composite gas flood: CO_2 followed by N_2 foam (injection gas ratio 2:1), an injection speed of 140 t/d, an injection volume of 0.31 PV, and an injection–production ratio of 3.2. This scheme predicts a cumulative oil production of 3.51×10^5 t and a fractal dimension of 1.672, with numerical simulation confirming minimal deviations (<1%) from predictions.

The 140 t/d injection rate, differing from the single-factor optimum, results from global optimization that captures critical parameter interactions, highlighting the need for a holistic approach.

5.2. Implications for Field Application

For field application, the proposed optimal scheme demonstrates strong operational feasibility and economic potential. The specified injection parameters, including the 140 t/d speed and 0.31 PV volume, are within the operational envelope of standard gas and foam injection facilities, requiring no exceptional technological advancements. From an economic perspective, the substantial incremental oil recovery (4.89% increase, adding 3.17×10^4 t of oil) is projected to economically justify the costs associated with gas procurement, foam agent, and process implementation. A preliminary cost–benefit analysis indicates that the projected oil revenue significantly outweighs the incremental operational and capital expenditures, underscoring the financial viability of the project.

Furthermore, the optimization methodology provides a transferable framework for scaling up the application. The workflow integrating numerical simulation, fractal characterization, and sensitivity analysis can be adapted to optimize development strategies for similar blocks within the same field or analogous bottom-water sandstone reservoirs. This offers a practical and systematic strategy for enhancing full-field development, moving beyond single-well or single-pilot-scale optimization. The use of the fractal dimension as a quantitative metric for coning control effectiveness provides field engineers with a clear and novel indicator to monitor and guide the flooding process towards more stable displacement and higher recovery.

5.3. Limitations and Future Perspectives

The study's findings should be considered in light of its limitations, which can be categorized as scientific and practical.

Scientific limitations: The analysis employed a static set of parameters. It does not explore dynamic adjustment strategies during the long-term development process, which might unlock additional recovery potential. Furthermore, uncertainties in key reservoir properties, such as permeability distribution, were not quantified. These uncertainties could influence the precise sensitivity rankings of the injection parameters.

Practical limitations: The economic thresholds for key parameters, particularly the cost–benefit trade-offs of larger injection volumes or higher gas ratios, require more precise quantification. Additionally, the successful field application of this fractal-based coning control strategy would necessitate the integration of a real-time monitoring and control system, which was beyond the scope of this study.

Looking forward, this research opens two promising avenues. First, fractal theory could be integrated with machine learning. A real-time monitoring system could be devel-

oped to invert the fractal dimension from production data, enabling dynamic forecasting and early warning of water coning. Second, the methodology shows potential for application in carbonate reservoirs. However, a successful transition would require adapting the fractal model to characterize the more complex and heterogeneous fracture–vuggy systems typical of carbonates, moving beyond the sandstone case studied here.

6. Conclusions

This study introduces an integrated workflow combining numerical simulation, fractal theory, and sensitivity analysis to optimize composite gas flooding in bottom-water sandstone reservoirs. The principal conclusions are as follows.

A novel fractal-based characterization method was established for quantifying water coning dynamics. This research pioneers the application of fractal dimensions to quantitatively characterize the morphology of the bottom-water cone during gas flooding. This metric provides a more rigorous and quantitative evaluation of coning control effectiveness, moving beyond traditional production data alone and offering a new tool for monitoring and optimizing displacement processes in the field.

The global optimization scheme significantly enhances oil recovery while effectively suppressing water coning. The optimal development strategy for the studied reservoir is a composite gas type involving CO_2 followed by N_2 foam, with an injection gas ratio of 2:1, an injection speed of 140 t/d, an injection volume of 0.31 PV, and an injection–production ratio of 3.2. This holistically optimized scheme, which supersedes single-factor results by accounting for critical parameter interactions, is projected to achieve a recovery factor of 39.52% over 15 years—an increase of 4.89%—while reducing the fractal dimension to 1.672, indicating superior coning control.

Parameter sensitivity analysis reveals distinct and complementary control mechanisms. The study identifies a clear functional decoupling: The injection gas ratio is the most sensitive parameter for cumulative oil production, as it directly governs the balance between CO_2 miscible displacement and foam blocking. In contrast, the injection volume is paramount for suppressing water coning (as reflected by the fractal dimension), as it determines the scale and stability of the foam barrier. Their strong interaction necessitates coordinated optimization.

The proposed methodology presents a viable and transferable strategy for field application. The optimized parameters are operationally feasible with standard gas and foam injection facilities. The substantial incremental oil recovery is projected to justify the associated costs, demonstrating strong economic potential. Furthermore, the integrated workflow provides a practical and scalable framework for designing and optimizing development strategies in similar bottom-water reservoirs, with broader implications for advancing CO_2 utilization in enhanced oil recovery.

Author Contributions: Conceptualization, K.C. and B.L.; methodology, K.C. and X.Z.; software, K.C.; formal analysis, B.L.; resources, B.L. and X.Z.; data curation, K.C.; writing—original draft preparation, K.C.; writing—review and editing, B.L. and X.Z.; supervision, B.L. and X.Z.; funding acquisition, B.L. All authors have read and agreed to the published version of the manuscript.

Funding: This study was supported by the National Natural Science Foundation of China (52174019), and the National Science and Technology Major Project of the Ministry of Science and Technology of China (2025ZD1406407), (2025ZD1405902), and (2025ZD1407501).

Data Availability Statement: Data will be made available on request.

Acknowledgments: We thank Xiaojie Zheng for his help with data analysis.

Conflicts of Interest: Author Xiaojie Zheng was employed by the company Sinopec Group Northwest Petroleum Branch. The remaining authors declare that the research was conducted in the absence of any commercial or financial relationships that could be construed as a potential conflict of interest.

References

1. Li, Z.; Elsworth, D. Controls of CO_2–N_2 gas flood ratios on enhanced shale gas recovery and ultimate CO_2 sequestration. *J. Pet. Sci. Eng.* **2019**, *179*, 1037–1045. [CrossRef]
2. Li, Z.; Su, Y.; Shen, F.; Huang, L.; Ren, S.; Hao, Y.; Wang, W.; Meng, Y.; Fan, Y. Investigation of CO_2 storage and EOR of alternating N_2 and CO_2 injection using experiments and numerical simulation. *Fuel* **2023**, *340*, 127517. [CrossRef]
3. Fang, T.; Wang, M.; Gao, Y.; Zhang, Y.; Yan, Y.; Zhang, J. Enhanced oil recovery with CO_2/N_2 slug in low permeability reservoir: Molecular dynamics simulation. *Chem. Eng. Sci.* **2019**, *197*, 204–211. [CrossRef]
4. Yu, T.; Li, Q.; Hu, H.; Tan, Y.; Xu, L. Residual oil retention and stripping mechanism of hydrophilic pore surfaces during CO2 and N2 combined gas flooding. *J. Pet. Sci. Eng.* **2022**, *218*, 110989. [CrossRef]
5. Liu, P.; Zhang, X. Enhanced oil recovery by CO_2–CH_4 flooding in low permeability and rhythmic hydrocarbon reservoir. *Int. J. Hydrogen Energy* **2015**, *40*, 12849–12853. [CrossRef]
6. Cho, J.; Min, B.; Kwon, S.; Park, G.; Lee, K.S. Compositional modeling with formation damage to investigate the effects of CO_2–CH_4 water alternating gas (WAG) on performance of coupled enhanced oil recovery and geological carbon storage. *J. Pet. Sci. Eng.* **2021**, *205*, 108795. [CrossRef]
7. Wang, Z.-H.; Sun, B.-W.; Guo, P.; Wang, S.-S.; Liu, H.; Liu, Y.; Zhou, D.-Y.; Zhou, B. Investigation of flue gas water-alternating gas (flue gas–WAG) injection for enhanced oil recovery and multicomponent flue gas storage in the post-waterflooding reservoir. *Pet. Sci.* **2021**, *18*, 870–882. [CrossRef]
8. Bender, S.; Akin, S. Flue gas injection for EOR and sequestration: Case study. *J. Pet. Sci. Eng.* **2017**, *157*, 1033–1045. [CrossRef]
9. Han, H.; Li, S.; Ma, D.; Ji, Z.; Yu, H.; Chen, X. Investigation of flue gas displacement and storage after the water flooding in a full diameter conglomerate long-core. *Pet. Explor. Dev.* **2018**, *45*, 903–909. [CrossRef]
10. Kang, W.-L.; Zhou, B.-B.; Issakhov, M.; Gabdullin, M. Advances in enhanced oil recovery technologies for low permeability reservoirs. *Pet. Sci.* **2022**, *19*, 1622–1640. [CrossRef]
11. Tian, Y.; Uzun, O.; Shen, Y.; Lei, Z.; Yuan, J.; Chen, J.; Kazemi, H.; Wu, Y.-S. Feasibility study of gas injection in low permeability reservoirs of Changqing oilfield. *Fuel* **2020**, *274*, 117831. [CrossRef]
12. Monette, M.; Nguyen, Q.P. Investigation of the effect of gas compositions on low-tension-gas flooding. *J. Pet. Sci. Eng.* **2021**, *207*, 109140. [CrossRef]
13. Qazvini Firouz, A.; Torabi, F. Utilization of carbon dioxide and methane in huff-and-puff injection scheme to improve heavy oil recovery. *Fuel* **2014**, *117*, 966–973. [CrossRef]
14. Afzali, S.; Rezaei, N.; Zendehboudi, S. A comprehensive review on Enhanced Oil Recovery by Water Alternating Gas (WAG) injection. *Fuel* **2018**, *227*, 218–246. [CrossRef]
15. Al-Mudhafar, W.J.; Rao, D. Lessons Learned from the Field-Scale Simulation of the Gas-Assisted Gravity Drainage GAGD Process in Heterogeneous Sandstone Oil Reservoirs. In Proceedings of the SPE Western Regional Meeting, Bakersfield, CA, USA, 23–27 April 2017; p. D031S006R002.
16. Al-Mudhafar, W.J.; Rao, D.N.; Wojtanowicz, A.K. Leveraging Designed Simulations and Machine Learning to Develop a Surrogate Model for Optimizing the Gas–Downhole Water Sink–Assisted Gravity Drainage (GDWS-AGD) Process to Improve Clean Oil Production. *Processes* **2024**, *12*, 1174. [CrossRef]
17. Al-Mudhafar, W.J.; Rao, D.N.; Srinivasan, S. Reservoir sensitivity analysis for heterogeneity and anisotropy effects quantification through the cyclic CO_2-Assisted Gravity Drainage EOR process—A case study from South Rumaila oil field. *Fuel* **2018**, *221*, 455–468. [CrossRef]
18. Al-Obaidi, D.A.; Al-Mudhafar, W.J.; Al-Jawad, M.S. Experimental evaluation of Carbon Dioxide-Assisted Gravity Drainage process (CO2-AGD) to improve oil recovery in reservoirs with strong water drive. *Fuel* **2022**, *324*, 124409. [CrossRef]
19. Mahmoud, T.N.; Rao, D.N. Mechanisms and Performance Demonstration of the Gas-Assisted Gravity-Drainage Process Using Visual Models. In Proceedings of the SPE Annual Technical Conference and Exhibition, Anaheim, CA, USA, 11–14 November 2007; p. SPE-110132-MS.
20. Schmitt Rahner, M.; Halisch, M.; Peres Fernandes, C.; Weller, A.; dos Santos, V.S.S. Fractal dimensions of pore spaces in unconventional reservoir rocks using X-ray nano- and micro-computed tomography. *J. Nat. Gas Sci. Eng.* **2018**, *55*, 298–311. [CrossRef]
21. Jafari, A.; Babadagli, T. Estimation of equivalent fracture network permeability using fractal and statistical network properties. *J. Pet. Sci. Eng.* **2012**, *92–93*, 110–123. [CrossRef]
22. Gu, D.; Ding, D.; Gao, Z.; Zhang, A.; Tian, L.; Wu, T. Pressure transient analysis of multiple fractured horizontal wells in naturally fractured unconventional reservoirs based on fractal theory and fractional calculus. *Petroleum* **2017**, *3*, 326–339. [CrossRef]

23. Li, G.; Su, Y.; Wang, W. The fractal mathematical models for spontaneous and forced imbibition with different cross-section shapes in shale oil reservoir. *Fractals* **2023**, *31*, 2350002. [CrossRef]
24. Zhang, Q.; Wang, W.-D.; Su, Y.-L.; Chen, W.; Lei, Z.-D.; Li, L.; Hao, Y.-M. A semi-analytical model for coupled flow in stress-sensitive multi-scale shale reservoirs with fractal characteristics. *Pet. Sci.* **2024**, *21*, 327–342. [CrossRef]
25. Su, H.; Zhang, S.; Sun, Y.; Wang, X.; Yu, B.; Wang, Y.; Yu, M.; Yang, M.; Meng, W.; Yi, H.; et al. A comprehensive model for oil–water relative permeabilities in low-permeability reservoirs by fractal theory. *Fractals* **2020**, *28*, 2050055. [CrossRef]
26. Kumar, N.; Augusto Sampaio, M.; Ojha, K.; Hoteit, H.; Mandal, A. Fundamental aspects, mechanisms and emerging possibilities of CO2 miscible flooding in enhanced oil recovery: A review. *Fuel* **2022**, *330*, 125633. [CrossRef]
27. Tan, Y.; Li, Q.; Xu, L.; Ghaffar, A.; Zhou, X.; Li, P. A critical review of carbon dioxide enhanced oil recovery in carbonate reservoirs. *Fuel* **2022**, *328*, 125256. [CrossRef]
28. Wei, P.; Pu, W.; Sun, L.; Pu, Y.; Wang, S.; Fang, Z. Oil recovery enhancement in low permeable and severe heterogeneous oil reservoirs via gas and foam flooding. *J. Pet. Sci. Eng.* **2018**, *163*, 340–348. [CrossRef]
29. Zhang, Y.; Li, B.; Lu, T.; Li, Z.; Zeng, X.; Song, Y. Adaptation study on nitrogen foam flooding in thick reservoirs with high water cut and high permeability. *Colloids Surf. A Physicochem. Eng. Asp.* **2023**, *657*, 130539. [CrossRef]
30. Hou, J.; Luo, M.; Zhu, D. Foam-EOR method in fractured-vuggy carbonate reservoirs: Mechanism analysis and injection parameter study. *J. Pet. Sci. Eng.* **2018**, *164*, 546–558. [CrossRef]
31. Wang, Y.; Liu, H.; Chen, Z.; Wu, Z.; Pang, Z.; Dong, X.; Chen, F. A visualized investigation on the mechanisms of anti-water coning process using nitrogen injection in horizontal wells. *J. Pet. Sci. Eng.* **2018**, *166*, 636–649. [CrossRef]
32. Wei, P.; Pu, W.; Sun, L.; Wang, B. Research on nitrogen foam for enhancing oil recovery in harsh reservoirs. *J. Pet. Sci. Eng.* **2017**, *157*, 27–38. [CrossRef]
33. Li, Y.-B.; Pu, W.-F.; Wei, B.; Chen, Y.-F.; Bai, B.-J. The feasibility of CO_2 and N_2 injection for the Tahe fracture-cavity carbonate extra-heavy oil reservoir: An experimental study. *Fuel* **2018**, *226*, 598–606. [CrossRef]
34. Orr, F.M.; Taber, J.J. Use of Carbon Dioxide in Enhanced Oil Recovery. *Science* **1984**, *224*, 563–569. [CrossRef] [PubMed]
35. Talebian, S.H.; Masoudi, R.; Tan, I.M.; Zitha, P.L.J. Foam assisted CO_2-EOR: A review of concept, challenges, and future prospects. *J. Pet. Sci. Eng.* **2014**, *120*, 202–215. [CrossRef]
36. Davoodi, S.; Al-Shargabi, M.; Wood, D.A.; Mehrad, M.; Rukavishnikov, V.S. Carbon dioxide sequestration through enhanced oil recovery: A review of storage mechanisms and technological applications. *Fuel* **2024**, *366*, 131313. [CrossRef]
37. Yang, J.; Hou, J.; Qu, M.; Liang, T.; Wen, Y. Experimental study the flow behaviors and mechanisms of nitrogen and foam assisted nitrogen gas flooding in 2-D visualized fractured-vuggy model. *J. Pet. Sci. Eng.* **2020**, *194*, 107501. [CrossRef]

Disclaimer/Publisher's Note: The statements, opinions and data contained in all publications are solely those of the individual author(s) and contributor(s) and not of MDPI and/or the editor(s). MDPI and/or the editor(s) disclaim responsibility for any injury to people or property resulting from any ideas, methods, instructions or products referred to in the content.